Adv Syst Sci Appl 2020; **04**; 11-26
Published online at https://ijassa.ipu.ru.

Frequency-Geometric Identification of Magnetization Characteristics of Switched Reluctance Machine

Laila Kadi[1*], Adil Brouri[1], Abdelmalek Ouannou[1]

[1)] *IMSM Team, L2MC Laboratory, ENSAM, Moulay Ismail University, Meknes, Morocco*

E-mail: lailakadigi@gmail.com, a.brouri@ensam-umi.ac.ma, abdelmalekouannou@gmail.com

Abstract: Accurate modeling of electrical drives for online testing is a relevant problem. Switched Reluctance Machine (SRM) has lately attracted significant attention because it has several advantages compared to conventional engines. It is simple, free of rare-earth and fault-tolerant machine. An analytical model of a SRM has not been reported yet due to the dynamic and strong nonlinearity of SRM. The most SRM control and applications are based on several assumptions and simplifications. Therefore, it is convenient to develop an accurate approach to identify the SRM characteristics. In this paper, an analytical modeling and identification method of magnetization characteristics of Switched Reluctance Machine (SRM) is proposed. Presently, an exact mathematical model of SRM is established. Unlike several previous studies, in this approach the system nonlinearities of SRM are allowed to be hysteresis (i.e. the hysteresis effect is considered) and taking account the inherent magnetic nonlinearity. Indeed, the SRM is considered as highly nonlinear which makes the modeling of these machines difficult to achieve. Then, it is convenient to develop an accuracy model of SRM because it is always operated in the magnetically saturated mode to maximize the energy transfer. The developed model can be used in control, simulation and design development. Furthermore, an identification method, at standstill test, based on frequency technics is developed allowing the identification of SRM nonlinearities (considering the saturation and the hysteresis effects). In this respect, it is shown that the nonlinear behavior of SRM can be exactly described by a block-oriented nonlinear structure. Specifically, the SRM can be described by a Wiener nonlinear model. Compared to the existing methods, the proposed study gives good accuracy of flux-linkage value characteristics and enjoys the simplicity of implementation.

Keywords: switched reluctance machine, hysteresis effect, saturation effect, nonlinear identification, nonlinear modeling, Wiener model, frequency-geometric method

1. INTRODUCTION

The world is now focused on how to reduce the cost of equipment used in renewable energy, electrical vehicles (EV), as well as in other applications. For wind energy conversion, many research has been done to evaluate the generator that is characterized by low cost, easy to maintain, high performance, and able to work under variable speeds [1, 2]. Moreover, the choice of motor drives for EV is very critical. In this context, the SRM is typically selected as a generator or motor because of its low cost, simplicity, robust structure, small moment of inertia rotor and fault-tolerant capability. Then, it is easy to maintain. Note that the majority of losses show up in the stator because the SRM has no rotor winding, no brushes, and does not have a magnet permanent [3] (see Fig. 1), there are also others benefits of SRM. In view of these significant remarks, the SRM is relatively easy to cool and is insensitive to high temperatures [4]. The SRM can be a suitable choice for wind energy and EV applications. In this respect, the SRM becomes more competitive compared to the classical machines such as induction machines. However, its major defects are torque ripples and acoustic noise [4]. Note that several studies are still ongoing to mitigate these effects [5, 6].

[*] Corresponding author: lailakadigi@gmail.com

Even though the several advantages of the SRM, the strong nonlinearity makes the modeling of SRM not an easy task. Despite all efforts in modeling and identification of SRM, finding an analytical model, which can accurately represent the nonlinear behavior of SRM, is widely open for scientific research. As commonly used in the literature, the modeling and identification methods of SRM flux linkage or self-inductance characteristics are classified into 4 categories: experimental measurements [7, 8], numerical solutions [9, 10], intelligent methods [11, 12], and analytical approaches [13, 14].

Roughly, the experimental methods are costly, require considerable time, can damage the machine and possibly create a safety hazard. Therefore, this method can be used to validate the obtained results.

Previous research has shown that two magnetization characteristics have been generally looked for SRM modeling. The first method is established using the inductance characteristics based model. The second solution is based on the flux-linkage [4]. At this stage, it is worth emphasizing the difficulty to establish a model that can accurately describe the behavior of the machine. This study proposes the development of an exact analytical model for the SRM, which is featured by a simple structure and reduced computational time. Then, an identification method is proposed for determining the flux linkage magnetization characteristics.

Lately, researchers have shown an increased interest in using block-oriented nonlinear models based on the input and output systems [16–18]. In this paper, it is proved that the SRM behavior can be accurately designed using block-oriented nonlinear model. Specifically, it is shown that the SRM at standstill can be exactly described by the Wiener model (Fig. 2). This later is given by the cascade connection of a linear dynamic system followed by a static or dynamic nonlinearity block [17, 18] as shown in Fig. 2. To the author's knowledge, for the first time, it has been shown that the SRM can be exactly described by the Wiener model.

As soon as a model of SRM is obtained, the identification method of the system parameters using this model constitutes also an important problem. In this article, a new approach is suggested for the identification of the magnetization characteristics often called flux linkage characteristics are much dependent on current and rotor position of the motor. Note that the problem of identifying the SRM nonlinearities will be carried out including saturation and hysteresis effects. Presently, a frequency-domain solution is designed to determine the SRM nonlinearities. The frequency identification methods have been widely used to identify the nonlinear systems parameters [16, 19, 20]. It is shown that the SRM can be analytically described by a nonlinear system of Wiener model. The proposed frequency approach consists of applying a sine input voltage $v(t) = V\sin(\omega t)$ to the phase winding, for any given rotor position. Then, by recording the current measurement at the winding terminal, the system nonlinearities of the model describing the SRM can be identified using a simple Frequency-Geometric method. Then, the SRM can be modeled analytically using the data acquisition obtained by the finite element method (FEM).

Note that this study is quite different from previous works [21–24]. The first key step in the development of this identification approach is the determination of an accurate model describing the nonlinear behavior of SRM. Another key step consists of designing an identification method using an appropriate excitation signal to estimate the parameters and the characteristics of SRM. Then, the system nonlinearities of SRM are allowed to be static or hysteretic operator. Furthermore, the model and the identification solution take into account the inherent magnetic nonlinearity. Then, using the developed nonlinear model of SRM, an identification method at standstill test is developed. The identification approach is based on frequency technics using simple sine input voltage. It is shown that the inner signal of the SRM model can be analytically determined at any time t.

In the first stage, the hysteresis effect is not considered. A filtering algorithm of the current at the winding terminal is suggested. Accordingly, the system nonlinearities of the model describing the SRM can be easily identified using the recording of the phase current (the filtered signal) over one half-period of time. Then, the flux-linkage characteristics can be easily obtained. Furthermore, these results are compared with those obtained using magnetostatic method.

In the second stage, the saturation and the hysteresis effects of SRM nonlinearities are considered. For any given rotor position, the SRM phase winding is excited using also a sine input voltage. Then, using the proposed filtering algorithm of the phase current, the system nonlinearities of the model describing the SRM can be accurately estimated using the recorded data over one period of time. Accordingly, the flux-linkage characteristics can be provided without any other experiment (using uniquely the phase voltage and the recorded current). Compared to the magnetostatic method, it is shown that the proposed study gives good accuracy of flux-linkage value characteristics, enjoys the simplicity of implementation and characterized by a reduced computational time. To the authors' knowledge, no previous study has found an exact model simulating the behavior of SRM. In addition, very few published works have attempted to identify the hysteresis operator.

The paper is organized as follows: The principle of operation and the equations describing the SRM are stated in Section 2. Then, the mathematical model and the description of the identification method of SRM nonlinearity are dealt within Section 3. Section 4 presents examples of obtained results using the proposed study.

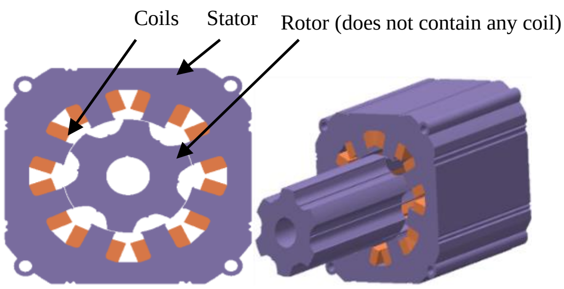

Fig. 1.1. Example of a 8/6 SRM

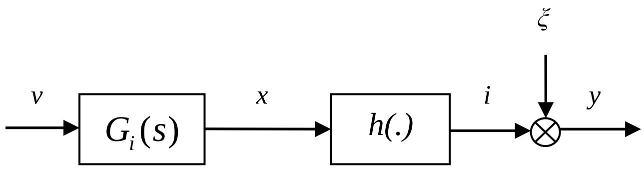

Fig.1.2. Wiener Model

2. OPERATION PRINCIPLE AND EQUATIONS DESCRIBING SRM

SRM is a double saliency device in which the stator comprises a salient magnetic circuit provided with coils supplied by a current *i*, and the rotor is also a salient ferromagnetic circuit but without any conductor or magnet [24], [25] as shown in Fig.1.1. In such machine, torque is produced by the tendency of its rotor to move to a position where the reluctance of the excited winding is minimized (aligned position) [24], [25]. Then, the machine rotates the magnetic field by synchronizing continuously and consecutively the supply of different phases with the rotor position by means of the firing angles (turn-on and turn-off). SRM can operate as a motor or generator. In order to obtain motoring mode, a stator phase is excited when the rotor is moving from an unaligned position towards the aligned position. Likewise, by exciting a stator phase when the rotor is moving from aligned towards the unaligned position, a generating mode will be attained [26]. To feed each stator phase of the SRM, we generally use an asymmetric half-bridge converter [27], [28] (Fig.2.3).

The magnetic flux created by the ampere-turns *Ni* oscillates between two extreme values correspond to [29]:

- Unaligned position in which the magnetic circuit has a maximum reluctance (minimum inductance) as illustrated by Fig. 2.4a.

- Aligned position in which the magnetic circuit has a minimum reluctance (maximum inductance) as explained by Fig. 2.4b.

The structure of the studied machine is of four phase *8/6* SRM, where *8* designates the number of poles in the stator (*Ns*) and 6 is the number of poles in the rotor (*Nr*). The choice of *Ns* and *Nr* is important since they have significant implications on the torque. The material of the SRM stator and rotor is steel M36 with the nonlinear B-H characteristic.

The mutual coupling between adjacent phases is very small and can be neglected[25], [29]. Let i, R, L, ω, θ, and v denote the phase current, phase resistance, inductance, rotor speed, rotor position angle, and phase voltage respectively. Then, the voltage equation of a phase winding can be given as:

$$v(t) = R\,i(t) + \frac{d\lambda(\theta,i)}{dt} \tag{2.1}$$

where λ is the flux-linkage per phase. Under the hypothesis of nonmagnetic coupling between phases (at any given time, only one phase is excited), the flux-linkage can be expressed as follows:

$$\lambda(\theta,i) = L(\theta,i)\,i \tag{2.2}$$

Due to the nonlinear behavior of the ferromagnetic material, the flux in the stator phases varies nonlinearly according to the rotor position θ and the phase current i. Accordingly, through direct derivation of (2.2) in (2.1), one immediately gets the following expression of the phase voltage:

$$v(t) = R\,i(t) + L(\theta,i)\frac{di}{dt} + i\left(\frac{\partial L(\theta,i)}{\partial i}\frac{di}{dt} + \omega\frac{\partial L(\theta,i)}{\partial \theta}\right) \tag{2.3}$$

The last term in (2.3) is the back electromotive force (EMF) voltage that is expressed by:

$$e = \omega\, i\,\frac{\partial L(\theta,i)}{\partial \theta} \tag{2.4}$$

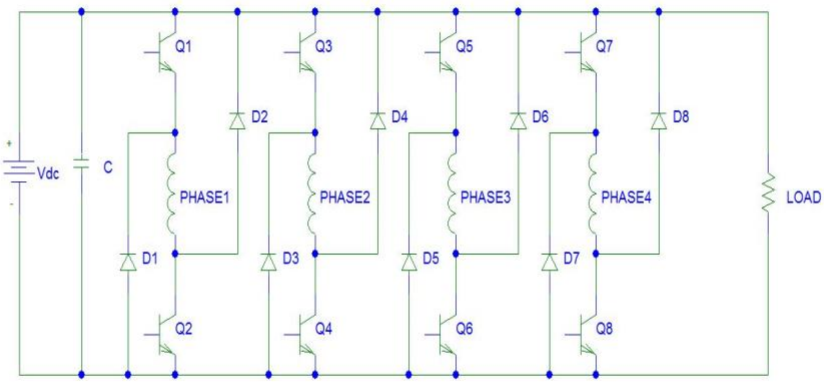

Fig.2.3. Asymmetric Half Bridge Converter

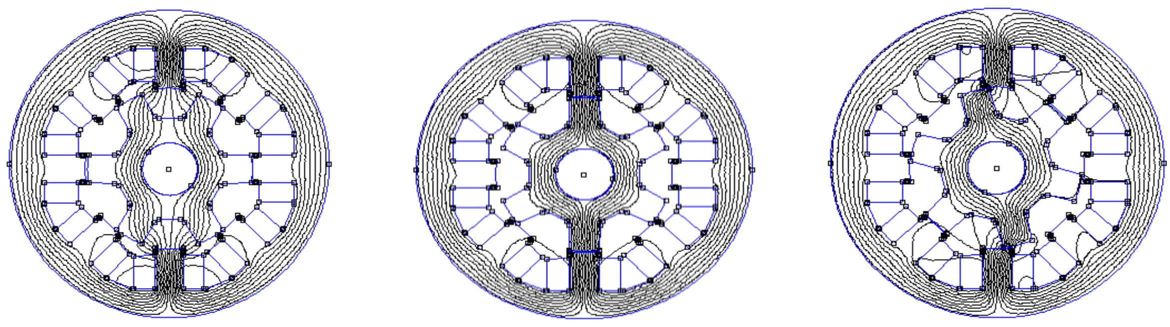

Fig.2.4 (a) Unaligned position; (b) Aligned position; (c) Midway position

3. MODELING AND IDENTIFICATION APPROACH OF SRM

At standstill test, the back electromotive force (EMF) voltage is nil because it is proportional to the shaft speed. Accordingly, the expression of phase voltage in (2.3) becomes:

$$v(t) = R\,i(t) + L(\theta,i)\frac{di}{dt} + i\,\frac{\partial L(\theta,i)}{\partial i}\frac{di}{dt} \tag{3.1}$$

The rotor of SRM is blocked at specific positions relative to the phase to be tested, e.g. at aligned, unaligned, and a midway between the above two positions. At blocked rotor (for any given rotor position θ), the nonlinearity $L(i)\big|_{\theta}$ (i.e. the inductance according to the current phase) can be described using a finite orthogonal function, e.g. polynomial decomposition [30], [31]:

$$L(i)\big|_{\theta} = \sum_{k=0}^{n} a_k i^k \tag{3.2}$$

where n is the polynomial function degree and a_k its coefficients. Then, it is readily follows from (3.1) and (3.2) that the phase voltage can be expressed as:

$$v(t) = \frac{d}{dt}\left(\sum_{k=0}^{n} b_k i^{k+1}\right) \tag{3.3a}$$

where:

$$b_k = \begin{cases} \dfrac{R}{2} + a_1 & for \quad k = 1 \\ a_k & for \quad k \neq 1 \end{cases} \tag{3.3b}$$

This result means that the phase voltage can be obtained by deriving a polynomial function according to the phase current. Then, let introduce the following polynomial function:

$$f(i) = \sum_{k=0}^{n} b_k i^{k+1} \tag{3.4a}$$

Then, in view of (3.4a), it follows that the phase voltage $v(t)$ in (3.3a) can be rewritten as follows:

$$v(t) = \frac{df(i)}{dt} \tag{3 .4b}$$

Remark 3.1:

It follows from the formulae (3.2)-(3.4) show that the nonlinear system having, the phase current $i(t)$ as input and the phase voltage $v(t)$ as output, can be described by a Hammerstein model, i.e., nonlinear element ($f(i)$) followed by a linear block (derivative term).

At this point, it is worth emphasizing that the derivative action can be modeled by a linear block. It is readily follows that the analytical nonlinear system (3.4a-b) (the phase voltage *v(t)* according to the phase current *i(t)* for any given rotor position) can be modeled by a nonlinear subsystem followed by a linear dynamical element as shown by Fig.3.1. This nonlinear model is called Hammerstein system.

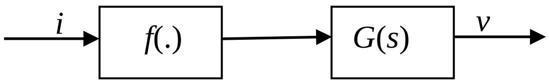

Fig. 3.1. Hammerstein nonlinear model

The aim presently is to develop an identification approach allowing to estimate the inductance nonlinearity $L(i)\big|_{\theta}$, for any given rotor position θ , and the flux-linkage $\lambda(\theta,i) = L(\theta,i)\,i$. Furthermore, the hysteretic shape of the flux linkage can be seen.

Then, it is worth emphasizing that, from practical point of view, the input signal of SRM is not a current excitation, but rather a phase voltage and the output signal of SRM is the phase current.

Indeed, the SRM is generally excited by a phase voltage and the phase current can be viewed as the output measurement. Then, the output electrical signal of SRM (i.e. the phase current *i(t)*) according to the input excitation (i.e. the phase voltage *v(t)*) can be modeled by a nonlinear system of Wiener model (Fig.1.2), where *h(.)* is the system nonlinearity, $G_i(s)$ is the linear subsystem and *ξ(t)* is the measurement noise. Specifically, the linear element is an integrator block ($G_i(s) = 1/s$). The above model is analytically described by the following equations:

$$x(t) = g_i(t) * v(t) \tag{3.5}$$

$$i(t) = h\big(x(t)\big) \tag{3.6}$$

$$y(t) = i(t) + \xi(t) \tag{3.7}$$

where: $g_i(t) = \int_0^{+\infty} G_i(s)e^{st}ds$ (the inverse Laplace Transform of $G_i(s)$); the symbol '*' refers to the convolution operation; *v(t)* and *y(t)* represent the (measurable) input and output of the system, respectively. In this respect, note that the internal signal *x(t)* is not accessible to measurement. At this stage, an identification approach is proposed based on frequency method. Then, the SRM characteristics and the parameters determination can be dealt using frequency-geometric tools. Accordingly, the following sine signal is being applied to the system input (phase voltage):

$$v\big(t\big) = V\sin(\omega t) \tag{3.8}$$

In the steady state, the internal signal *x(t)* is also sinusoidal (of the same period of *v(t)*) and can be written as [15], [16], [18]:

$$x(t) = -(V/\omega)\cos(\omega t) \tag{3.9}$$

Commonly, the main complexity of Wiener model identification problem is due to the fact that the internal variable *x(t)* is not accessible to measurement. Fortunately, in our nonlinear model, it follows (3.9) the inner signal *x(t)* can be easily estimated at any time *t*. Presently, a frequency domain method is proposed to identify the system nonlinearity *h(.)* using the data obtained from finite element method. In this respect, the sinusoidal voltage $v(t) = V\sin(\omega t)$ is being applied to the phase winding and the resulting phase current is recorded. Then, the SRM nonlinearities characteristics can be accurately determined using only the system input (i.e. the phase voltage *v(t)*) and the measurable output signal (i.e. the phase current *i(t)*). It is interesting to bear in mind that, if the input excitation *v(t)* is *T=2π/ω*-periodic, then the steady state of inner signal *x(t)* and output system *i(t)* are also periodic of the same period *T* as *v(t)* [15], [18]. This result is a quite interesting achievement as it shows that, the curve of *i(t)* according to *x(t)* can be easily obtained using uniquely the set of points $\left(x(t),\ i(t)\right) = \left(\text{-}(V/\omega)\cos(\omega t),\ i(t)\right)$, in the steady state, over one period *T*. The determination of the functions $\left(x(t),\ i(t)\right) = \left(-(V/\omega)\cos(\omega t),\ i(t)\right)$ constitutes another key challenge of this work, because it makes possible the estimation of nonlinearity *h(.)* of SRM model (Fig. 1.2) at any given rotor position θ.

Practically speaking, the useful information (the phase current *i(t)*) is not directly accessible to the measurement. Indeed, the measurement signal *y(t)* is the phase current with additive noise (please see (3.7)). Let $\hat{i}_M(t)$ denotes the phase current estimate. In this respect, thanks to periodicity of *i(t) (T=2π/ω)*, an accurate estimate of the phase current can be obtained using the following estimator:

$$\hat{i}_M(t) \overset{def}{=} \frac{1}{M}\sum_{k=0}^{M-1} y\left(t + 2\pi k/\omega\right) \text{ for } t \in \left[0\ \ 2\pi/\omega\right) \tag{3.10a}$$

$$\hat{i}_M(t + 2\pi k/\omega) = \hat{i}_M(t) \qquad \textit{otherwise} \tag{3.10b}$$

where M is an integer, preferably of large value. Then, the identification of the system nonlinearity *h(.)* can easily be achieved using the collected data over the interval $\left[0\ \ 2\pi M/\omega\right)$. For convenience, let us summarize the identification steps of system nonlinearity *h(.)*:

Firstly, using the set of recorded data $\left\{y(t);\ \textit{for}\ t \in \left[0\ \ MT\right)\right\}$, the estimate of the current phase *i(t)* can be obtained using the estimator (3.10a-b). Then, we generate the fictive internal signal $x(t) = -(V/\omega)\cos(\omega t)$ over one period *T*. Therefore, the estimate $\hat{h}_M(.)$ of nonlinear element *h(.)* can be simply performed by constructing the set of points: $\left\{\left(x(t),\ \hat{i}_M(t)\right);\ \textit{for}\ t \in \left[0\ \ T\right)\right\}$.

Finally, an accurate estimate of SRM nonlinearity, for different rotor positions, can be obtained using the above frequency-geometric method. The above results lead to the following proposition.

Proposition 3.1:

Let consider the identification problem of SRM model at standstill (Fig. 1.2), where the noise $\xi(t)$ is supposed to be a zero-mean ergodic stochastic process. This latter is excited by the sine input $v(t) = V\sin(\omega t)$. Accordingly, one has with probability 1 (w.p.1):

1. The current estimate $\hat{i}_M(t)$ converges to the true phase current signal *i(t)*.

2. The system nonlinearity estimate $\hat{h}_M(.)$ converges to the true function *h(.)*.

Proof.

To prove the first part of the proposition, let us combining (3.7) and (3.10a-b), one thus gets:

$$\hat{i}_M(t) = \frac{1}{M}\sum_{k=0}^{M-1} i\left(t + 2\pi k / \omega\right) + \frac{1}{M}\sum_{k=0}^{M-1} \xi(t + 2\pi k / \omega) \tag{3.11}$$

Bearing in mind that the phase current *i(t)* is $T=2\pi/\omega$ -periodic, (3.11) can thus be rewritten as:

$$\hat{i}_M(t) = i(t) + \frac{1}{M}\sum_{k=0}^{M-1} \xi(t + 2\pi k / \omega) \tag{3.12}$$

Using the fact that the noise is a zero-mean ergodic stochastic process, the last term in (3.12) converges to zero as M tends to infinity (w.p.1). This completes the first part of proposition.

To prove the second part of proposition, let us recall that for the input $v(t) = V\sin(\omega t)$ (Fig.1.2), the inner signal *x(t)* belongs to the interval $[-V/\omega \;\; V/\omega]$. Accordingly, the system nonlinearity *h(.)* can be described, within the interval $[-V/\omega \;\; V/\omega]$, as the set of all points $\left\{\left(x(t),\, i(t)\right) = \left(x(t),\, h\left(x(t)\right)\right);\; t \in \left[0 \;\; T\right)\right\}$. Therefore, the nonlinearity estimate $\hat{h}_M(.)$ can be featured by plotting the set of points $\left\{\left(x(t),\, \hat{i}_M(t)\right);\; t \in \left[0 \;\; T\right)\right\}$. It follows from the first part of proposition that:

$$\lim_{M\to\infty} \left(x(t),\, \hat{i}_M(t)\right) = \left(x(t),\, h(x(t))\right) \textit{ for any } t \in \left[0 \;\; T\right) \tag{3.13}$$

This means that the nonlinearity estimate $\hat{h}_M(.)$ converges to the true function *h(.)* w.p.1 for any $t \in \left[0 \;\; T\right)$. This completes the proof of proposition.

This result is a quite interesting achievement as it shows that, it is possible to obtain an accurate estimate of SRM characteristics for any given rotor position θ. At this stage, other significant results can be observed. On one hand, if the system nonlinearity *h(.)* is static, the estimate $\hat{h}_M(.)$ of *h(.)* can be done by using simply the set of points $\left(x(t),\, \hat{i}_M(t)\right)$ over one-half period $t \in \left[0 \;\; T/2\right)$. On the other hand, in the case where the nonlinear element *h(.)* of SRM is hysteresis, the system nonlinearity estimate $\hat{h}_M(.)$ can be featured using the set of points $\left(x(t),\, \hat{i}_M(t)\right)$ over one period of time (i.e. $\left\{\left(x(t),\, \hat{i}_M(t)\right);\; \textit{for } t \in \left[0 \;\; T\right)\right\}$). These results lead to the following proposition.

Proposition 3.2:

Let us reconsider the above identification problem of SRM model (Fig. 1.2). This machine is excited by the phase voltage (3.8), where the amplitude V and the frequency *ω (rd/s)* of *v(t)* are kept constant. Let's assume that, in steady state, $h\left(x(kT)\right) = h\left(x((k+1)T)\right)$. Then, the following results are obtained:

1. If the hysteresis effect of SRM magnetization characteristics is not considered, for $x \in [-V/\omega \;\; V/\omega]$ the nonlinear element *h(.)* (in the steady state) can be constructed by fitting the set of points *(x(t), i(t))* over one half-period ($\textit{for } t \in \left[0 \;\; T/2\right)$).

2. Now, the hysteresis effect of SRM magnetization characteristics is considered. Then, for any fixed *V* and ω, the hysteretic nonlinearity *h(.)* (in the steady state) can be obtained by plotting the set of points $\{(x(t),\, i(t));\, t \in [0\ T)\}$ (i.e. over one period of time).

Proof.

First, one immediately gets using (3.6) -(3.9) for any $t \in [0\ T)$:

$$i(t) = h\big(x(t)\big) = h\big(-(V/\omega)\cos(\omega t)\big) \tag{3.14}$$

Then, if the SRM system nonlinearity *h(.)* is static (does not contain the hysteresis effect), then for any $t \in [0\ T/2)$ there exists $t' = T - t$ such that:

$$i(t) = h\big(x(t')\big) = h\big(x(t)\big) \ and \ t' \in [T/2\ T) \tag{3.15}$$

Accordingly, the static nonlinear function *h(.)* can be described uniquely by the set of points $\{(x(t), i(t));\, t \in [0\ T/2)\}$. This completes the first part of proposition.

At this stage, the function *h(.)* is hysteretic nonlinear operator. Accordingly, using the assumption $h\big(x(kT)\big) = h\big(x((k+1)T)\big)$ one immediately gets that all points of coordinates $\{(x(t), i(t));\, t \in [0\ T)\}$ build a closed locus [16], [18]. Furthermore, for any given amplitude *V* and frequency *ω*, a single closed locus is obtained. Finally, the shape of hysteretic nonlinearity h(.), for fixed values of *(V, ω)*, can be described by plotting the points of coordinates *(x(t), i(t))* for $t \in [0\ T)$.

Presently, the aim is to present a method of modeling and identification of the flux-linkage $\lambda(\theta, i)$. The above obtained achievement is useful to determine the flux-linkage features. Accordingly, it is readily follows from (2.1) that, the flux-linkage $\lambda(\theta, i)$ can be expressed as:

$$\lambda(\theta,i) = \int\big(v(t) - R\ i(t)\big)dt \tag{3.16}$$

Then, it follows from (3.9) and (3.16) that, the flux-linkage can be rewritten as:

$$\lambda(\theta,i) = -\frac{V}{\omega}\cos(\omega t) - \int R\ i(t)\,dt \tag{3.17}$$

$$\lambda(\theta,i) = x(t) - R\int h\big(x(t)\big)dt \tag{3.18}$$

where the first term part on the right side corresponds to *x(t)*, given by (3.9). Therefore, it readily follows from (3.17) that, the flux-linkage characteristics can be achieved using the resistor measurement *R*, the values of *x(t)* and the phase current measurement $\hat{i}_M(t)$. In this respect, it is worth emphasizing that no other information (experiment) is required to determine the flux-linkage characteristics. Indeed, the latter can be estimated using only the available information's in the first stage (i.e. $\hat{i}_M(t)$ and *x(t)*).

4. SIMULATION RESULTS & DISCUSSION

To show the efficiency of this approach, the machine *8/6* SRM is considered in simulations. Let us choose the rotor position $\theta = 0°$ as the aligned position of phase *A* (Fig. 2.4a). Accordingly, $\theta = 30°$ corresponds to the unaligned position of phase *A* (Fig. 2.4b) and $\theta = 15°$ corresponds to the Midway position. Simulations were carried out using a FEM software by collecting data acquisition at several specific positions (e.g. at aligned, midway and unaligned positions).

Firstly, the SRM is being excited by the sinusoidal phase voltage $v(t) = V\sin(\omega t)$, where the amplitude $V = 400V$ and the frequency $\omega = 314 rd/s$.

According to the proposition 3.2, note that the amplitude *V* and frequency ω *(rd/s)* of the input signal are kept constant. Accordingly, the steady state of phase current *i(t)* is also periodic of the same period of *v(t)*.

Furthermore, note that a noise signal $\xi(t)$ is added to the useful information (i.e. *i(t)*). This noise is supposed to be a zero-mean ergodic stochastic process. Then, the system output *y(t)*, i.e. the undisturbed phase current added to the measurement noise, is collected on the interval $t \in [0 \;\; MT)$, where *M=10*. Fig.4.1 illustrates *y(t)* for three rotor positions.

The plot confirms that the phase current measurement *y(t)* is also periodic of the same period of *v(t)*.

Then, using the estimator (3.10a-b), the phase current estimate $\hat{i}_M(t)$ can be obtained for any given rotor position. This latter is plotted in Fig. 4.2 over one period of time. It is clearly seen that, as the rotor gets closer to the aligned position, the saturation effect becomes more significant and notably distorts the shape of the phase current (the black curve in Fig. 4.2).

Bearing in mind that *x(t)* is not accessible to measurement, but it can be easily determined at any time *t* using the expression (3.9) (Fig. 1.2). Then, the nonlinearity estimate $\hat{h}_M(.)$ can be featured by the set of points $\{(x(t), \hat{i}_M(t));\, t \in [0 \;\; T)\}$ (using the phase current estimate $\hat{i}_M(t)$). At this stage, it is worth emphasizing that two cases can be observed according to the system nonlinearity *h(.)* (Proposition 3.2).

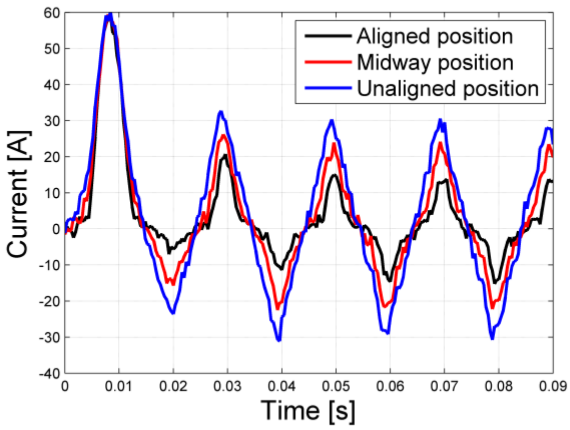

Fig. 4.1. Output signal $y(t)$

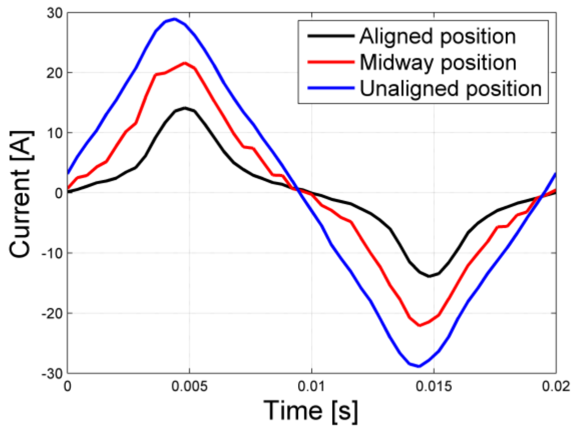

Fig. 4.2. Phase current estimate signal $\hat{i}_M(t)$

4.1. SRM magnetization characteristics without considering the hysteresis effect (static curves)

Presently, we suppose that *h(.)* is static nonlinearity. Then, the shape of *h(.)* can be described using the phase current estimate and the inner signal *x(t)* over one half-period (Proposition

3.2). Accordingly, an accurate estimate $\hat{h}_M(.)$ of the system nonlinearity *h(.)* can be obtained using the set of points $\{(x(t),\, \hat{i}_M(t));\, t \in [0\ \ T/2)\}$ (i.e. by plotting the phase current estimate $\hat{i}_M(t)$ in respect to *x(t)*). Then, the nonlinearity estimate $\hat{h}_M(.)$ for different rotor positions, e.g. aligned, midway and unaligned, can be achieved by repeating the same experiment. In this respect, the obtained nonlinearity estimate $\hat{h}_M(.)$ for aligned, midway, and unaligned positions are shown by Fig.4.3. The plots confirm that the function $\hat{h}_M(.)$ presents a severe nonlinearity at aligned position due to the saturation effect.

Then, another important feature of SRM is the flux-linkage, which is very interesting to be estimated. For convenience, let us consider the expression of flux-linkage $\lambda(\theta, i)$ in (3.17). Accordingly, this latter can be determined by integrating the estimated current and using the signal *x(t)* (given by (3.9)).

In this respect, it is worth emphasizing that the determination of flux-linkage features can be obtained using uniquely the results of experiments carried out in the first stage. In the case where the phase current is unidirectional, the first quadrant of *(λ, i)* plane is considered. Then, the obtained flux-linkage characteristics are shown in Fig.4.4. These results show that, using the proposed approach, the flux-linkage characteristics are acquired with good accuracy compared to those obtained using magnetostatic model.

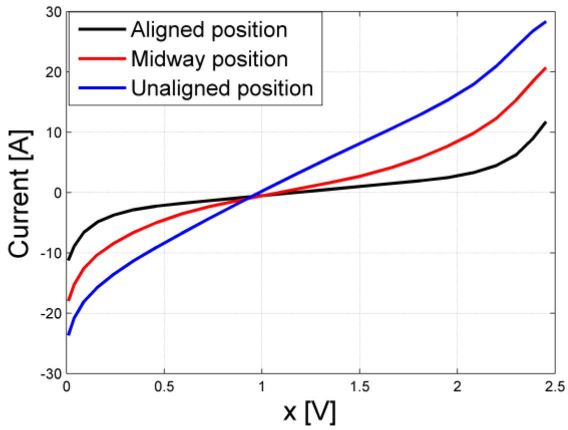

Fig. 4.3. The estimate of the function *h*(.) without taking into account the hysteresis effect

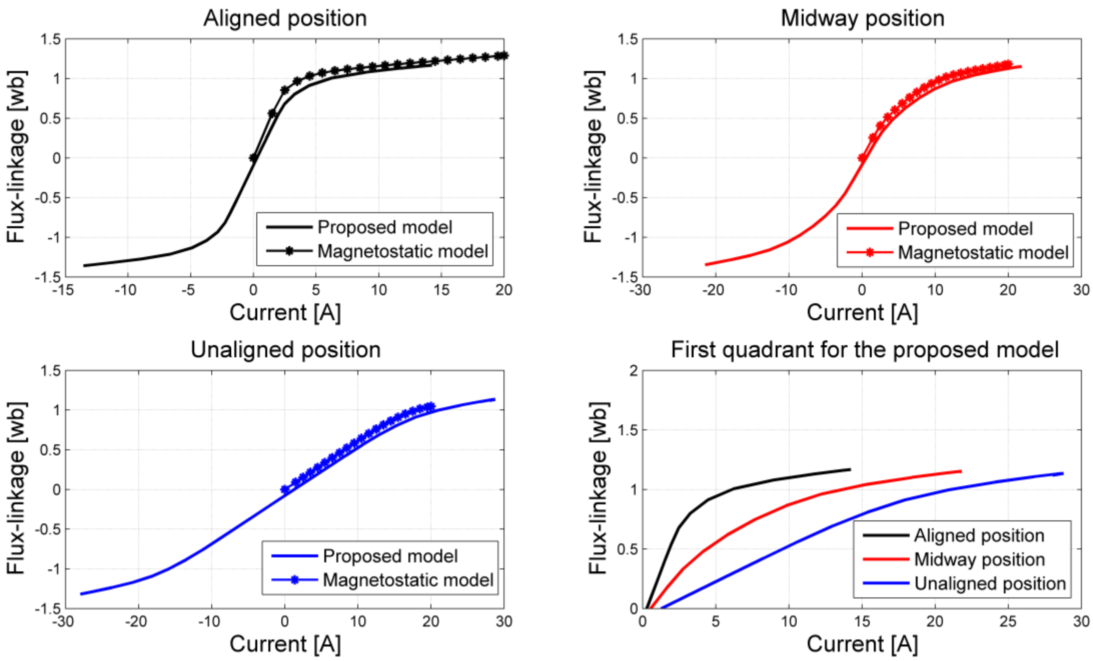

Fig. 4.4 Flux-linkage characteristics without considering hysteresis effect

4.2. SRM magnetization characteristics considering the hysteresis effect

Presently, the nonlinear elements are allowed to be hysteretic. To this end, a frequency-geometric tool is used as shown in section 3. In this respect, the determination of electrical nonlinearities and flux-linkage characteristics of SRM can be found using the same experiment suggested in the first case (without considering the hysteresis effect). Then, it follows Proposition 3.2 and using phase current estimate $\hat{i}_M(t)$, the hysteretic nonlinearity estimate $\hat{h}_M(.)$ can be featured by the set of points $\left(x(t), \hat{i}_M(t)\right)$ for $t \in \left[0 \;\; 2\pi/\omega\right)$. So, the curves of system nonlinearity estimate $\hat{h}_M(.)$ for three key positions (aligned, midway and unaligned positions) are shown by Fig.4.5. As can be seen, the obtained curves of $\hat{h}_M(.)$ are not static and are closer to closed locus (in steady state). These locus will be referred to the hysteretic behaviors of SRM. Furthermore, note that the surface of hysteretic curve increases according to the position rotor. Accordingly, the hysteretic losses are small at the aligned position and become high at the unaligned position.

.

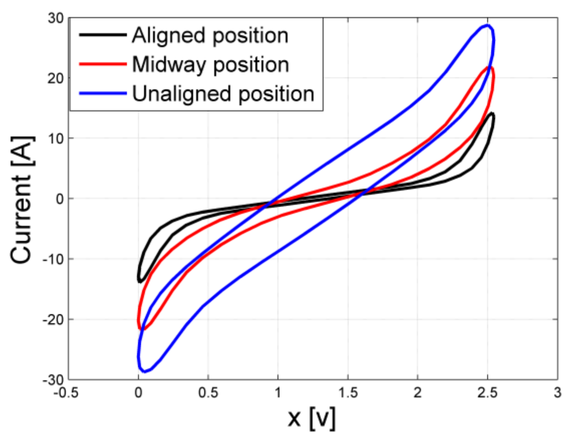

Fig. 4.5. The estimate of the function *h*(.) considering the hysteresis effect

In the case where the phase current is unidirectional, the first quadrant of (λ, i) plane is considered. Accordingly, the obtained flux-linkage $\lambda(\theta, i)$ characteristics are shown in Fig.4.6.

The achieved flux-linkage characteristics show that $\lambda(\theta, i)$ is not static, but it is close to a closed locus. Moreover, the hysteretic surface is considerably narrow at the aligned position and increases according to the position rotor.

Note that, the validation of the identification method was performed using magnetostatic technic as can be seen in Fig .4.4. Let us recall that, the magnetostatic method is a pure numerical solution which requires a full set of data obtained from FEM [25], [32]. This method differs substantially from our approach, which is based only upon the input-output measurement data. As can be seen in Fig.4.4, the achieved flux-linkage shapes using the proposed method and those obtained using magnetostatic give very close results. In the case where the hysteresis effect is considered, the present analysis confirms the existence of hysteresis effect, which is not too discussed in the literature.

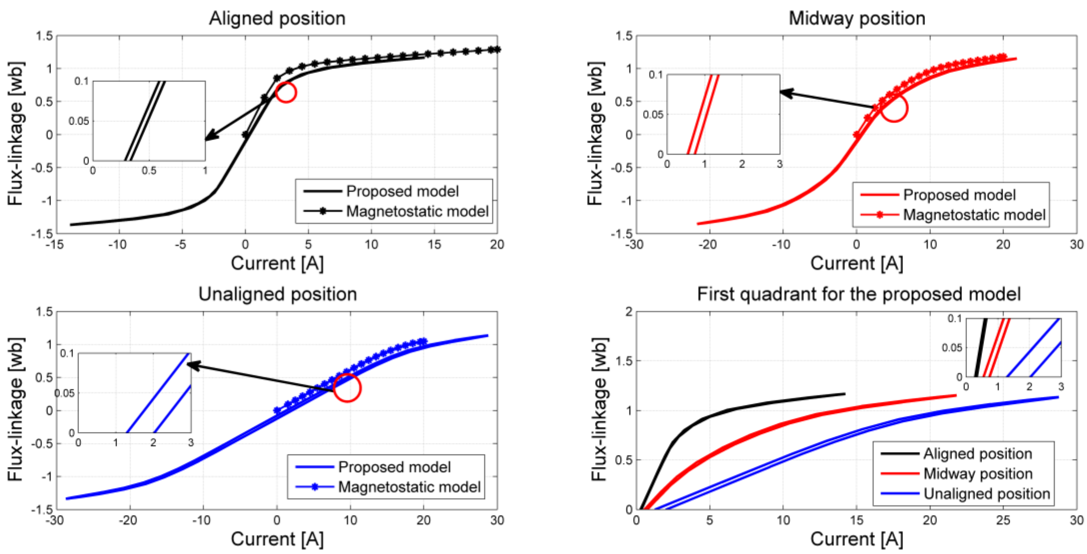

Fig. 4.6. Flux-linkage characteristics with hysteresis effect

5. CONCLUSION

This paper proposes an analytical modeling and identification method of magnetization characteristics of SRM. One key step in the design of such method is the construction of the nonlinear block-oriented model modelling the behavior of the SRM. Specifically, it is shown that the SRM can be described by a Wiener model. To our knowledge, no previous work has been dealt with this technic. Then, an analytical identification method is developed to obtain the magnetization characteristics of the SRM. The identification method is dealt based on a simple Frequency-Geometric method by applying a sine input voltage to the phase winding, for any given rotor position. Then, the inner signal $x(t)$ of the nonlinear Wiener system (the SRM model) can be easily estimated at any time t. Accordingly, all the electrical parameters of SRM can be accurately estimated using the phase voltage and the recording of the current measurement at the winding terminal.

On one hand, if the hysteresis effect of SRM nonlinearities is not considered, the magnetization characteristics can be estimated using data-acquisition over one-half period. The obtained results are compared with other achieved data using the FEM method. On the other hand, the identification of SRM magnetization features can be performed even if the hysteresis effect is considered using only data-acquisition over one period. In this respect, it is worth emphasizing that very few available works have attempted to identify the hysteresis effects of SRM.

Furthermore, it is shown that the hysteretic losses are generally small at the aligned position and can be of high value at the unaligned position. This result is confirmed by the area of the obtained hysteresis curve.

Another originality of the present study lies in the fact that the machine model can be analytically represented using block-oriented systems. The proposed Wiener model still be very simple in use and the magnetization characteristics can be easily achieved using the Frequency-Geometric method. Another feature of this work is the fact that the modeling design and the identification scheme require less computational time, unlike several previous studies. The accuracy of the model has been verified by comparing the obtained characteristics using this approach with those using the magnetostatic method.

Despite all efforts in modeling and identification of SRM, finding an accurate analytical model, which represents the nonlinear behavior of SRM, is wide open for scientific research. In terms of future work, it would be interesting to use the same model in real time. Then, this model can used to obtain the dynamical model of SRM. The hysteresis measurement (surface of the hysteretic curve) can offer some suggestions to handle the losses. This approach could be tested on some applications of SRM using the obtained model.

REFERENCES

1. R. Cardenas, R. Pena, M. Perez, J. Clare, G. Asher, and P. Wheeler, “Control of a Switched Reluctance Generator for Variable-Speed Wind Energy Applications,” *IEEE Transactions on Energy Conversion*, vol. 20, no. 4, 781–791, 2005.
2. D. A. Torrey, “Switched reluctance generators and their control,” *IEEE Transactions on Industrial Electronics*, vol. 49, no. 1, 3–14, 2002.
3. T. J. E. Miller, *Switched reluctance motors and their control*. Magna Physics , Oxford : Clarendon Press , New York : Oxford University Press., 1993.
4. A. Emadi, *Handbook of automotive power electronics and motor drives*. Taylor & Francis., 2017.
5. N. Saha, A. K. Panda, and S. Panda, “Speed control with torque ripple reduction of switched reluctance motor by many optimizing liaison technique,” *Journal of Electrical Systems and Information Technology*, vol. 5, no. 3, 829–842, Dec. 2018.
6. D. Marcsa and M. Kuczmann, “Design and control for torque ripple reduction of a 3-phase switched reluctance motor,” *Computers & Mathematics with Applications*, vol. 74, no. 1, 89–95, Jul. 2017.
7. T. A. S. Barros, P. J. S. Neto, M. V. Paula, A. B. Moreira, P. S. N. Filho, and E. R. Filho, “Automatic Characterization System of Switched Reluctance Machines and Nonlinear Modeling by Interpolation Using Smoothing Splines,” *IEEE Access*, 1–1, 2018.
8. M. V. Terzic, H. Li, B. Bilgin, and A. Emadi, “Comparison of Experimental Methods for Electromagnetic Characterization of Switched Reluctance Motors,” in *2018 XIII International Conference on Electrical Machines (ICEM)*, 2018, 1881-1888.
9. B. Parreira, S. Rafael, A. J. Pires, and P. J. CostaBranco, “Obtaining the Magnetic Characteristics of an 8/6 Switched Reluctance Machine: From FEM Analysis to the Experimental Tests,” *IEEE Transactions on Industrial Electronics*, vol. 52, no. 6, 1635–1643, Dec. 2005.

10. B. Ganji, M. Heidarian, and J. Faiz, “Modeling and analysis of switched reluctance generator using finite element method,” *Ain Shams Engineering Journal*, vol. 6, no. 1, 85–93, Mar. 2015.

11. O. Ustun, “A nonlinear full model of switched reluctance motor with artificial neural network,” *Energy Conversion and Management*, vol. 50, no. 9, 2413–2421, Sep. 2009.

12. X. Yao and Y. Yang, “Online modeling for switched reluctance motors using adaptive network based fuzzy inference system,” in *2017 29th Chinese Control And Decision Conference (CCDC)*, 2017, 1568-1573.

13. A. Khalil and I. Husain, “A Fourier series generalized geometry based analytical model of switched reluctance machines,” in *IEEE International Conference on Electric Machines and Drives, 2005.*, 2005, 490-497.

14. S. Li, S. Zhang, T. Habetler, and R. Harley, “Fast and accurate analytical calculation of the unsaturated phase inductance profile of 6/4 switched reluctance machines,” in *2016 IEEE Energy Conversion Congress and Exposition (ECCE)*, 2016, 1-8.

15. A. Brouri, L. Kadi, and S. Slassi, “Frequency identification of Hammerstein-Wiener systems with Backlash input nonlinearity.,” *International Journal of Control, Automation and Systems*, vol. 15, no. 5, 2222–2232, Oct. 2017.

16. F. Giri, A. Radouane, A. Brouri, and F. Chaoui, “Combined frequency-prediction error identification approach for Wiener systems with backlash and backlash-inverse operators,” *Automatica*, vol. 50, no. 3, 768–783, Mar. 2014.

17. F. Giri, Y. Rochdi, A. Radouane, A. Brouri, and F. Z. Chaoui, “Frequency identification of nonparametric Wiener systems containing backlash nonlinearities,” *Automatica*, vol. 49, no. 1, 124–137, Jan. 2013.

18. A. Brouri, F. Giri, F. Ikhouane, F. Z. Chaoui, and O. Amdouri, “Identification of Hammerstein-Wiener systems with Backlash input nonlinearity bordered by straight lines,” *IFAC Proceedings Volumes*, vol. 47, no. 3, 475–480, Jan. 2014.

19. A. Brouri, O. Amdouri, F. Z. Chaoui, and F. Giri, “Frequency identification of Hammerstein-Wiener systems with piecewise affine input nonlinearity,” *IFAC Proceedings Volumes*, vol. 47, no. 3, 10030–10035, Jan. 2014.

20. M. Aguado-Rojas, P. Maya-Ortiz, and G. Espinosa-Pérez, “On-line estimation of switched reluctance motor parameters,” *International Journal of Adaptive Control and Signal Processing*, vol. 32, no. 6, 950–966, 2018.

21. J. Hur, C. C. Kim, and D. S. Hyun, “Modeling of switched reluctance motor using Fourier series for performance analysis,” *Journal of Applied Physics*, vol. 93, no. 10, 8781–8783, May 2003.

22. Z. Peng, P. A. Cassani, and S. S. Williamson, “An Accurate Inductance Profile Measurement Technique for Switched Reluctance Machines,” *IEEE Transactions on Industrial Electronics*, vol. 57, no. 9, 2972-2979., Sep. 2010.

23. J. E. Stephen, S. K. Kumar, and J. Jayakumar, “Nonlinear modeling of a switched reluctance motor using LSSVM - ABC,” *Acta Polytechnica Hungarica*, vol. 11, no. 6, 143–158, 2014.

24. T.J.E. Miller, *Electronic control of switched reluctance machine*. New York : Oxford University Press, 1993.

25. K. Laila and B. Adil, “Nonlinear Numerical Study of Mutual Inductances for

Switched Reluctance Machine," 1–6, 2019.

26. A. Arifin, "Switched Reluctance Generator Drive in the Low and Medium Speed Operation : Modelling and Analysis," Massey University, 2013.

27. E. Darie and C. Cepişcă, "The use of Switched Reluctance Generator in wind energy applications," *2008 13th International Power Electronics and Motion Control Conference, EPE-PEMC 2008*, no. October 2008, 1963–1966, 2008.

28. S. Vukosavic and V. Stefanovic, "SRM inverter topologies: A comparative evaluation," *IEEE Transactions on Industry Applications*, vol. 27, no. 6, 1034–1047, 1991.

29. R. Krishnan, *Switched reluctance motor drives : modeling, simulation, analysis, design, and applications*. CRC Press, 2001.

30. Y. Sofiane, A. Tounzi, and F. Piriou, "A non linear analytical model of switched reluctance machines," *Applied Physics*, vol. 172, 163-172., 2002.

31. S. W. Zhao, N. C. Cheung, C. K. Lee, X. Y. Yang, and Z. G. Sun, "Survey of modeling methods for flux linkage of switched reluctance motor," in *2011 4th International Conference on Power Electronics Systems and Applications*, 2011, 1-4.

32. L. Kadi and A. Brouri, "Numerical Modeling of a Nonlinear Four-Phase Switched Reluctance Machine," in *2017 International Renewable and Sustainable Energy Conference (IRSEC)*, 2017, 1-6.

